JOURNAL OF Applied Polymer SCIENCE

Adsorption Removal of Crystal Violet from Aqueous Solution Using a Metal-Organic Frameworks Material, Copper Coordination Polymer with Dithiooxamide

Xiaojuan Li,[1] Lingyan Zheng,[2] Lianzhu Huang,[2] Ou Zheng,[2] Zhenyu Lin,[2] Longhua Guo,[2] Bin Qiu,[2] Guonan Chen[2]

[1]Department of Environment and Resources, Fuzhou University, Fuzhou, Fujian 350108, China
[2]MOE Key Laboratory of Analysis and Detection for Food Safety, Fujian Provincial Key Laboratory of Analysis and Detection Technology for Food Safety, Department of Chemistry, Fuzhou University, Fuzhou, Fujian 350002, China
Correspondence to: X. J. Li (E-mail: lixiaojuan@fzu.edu.cn) or Z. Y. Lin (E-mail: zylin@fzu.edu.cn)

ABSTRACT: The potential application of copper coordination polymer with dithiooxamide (H_2dtoaCu), one of the metal-organic frameworks (MOFs) in the adsorption removal of crystal violet (CV) from aqueous solution was studied. Batch adsorption experiments were carried out as a function of initial pH, adsorbent concentration, contact time, initial dye concentration and temperature. The adsorption of CV on H_2dtoaCu can be best described by the Langmuir isotherm model ($R^2 > 0.9983$) with maximum monolayer adsorption capacity of 165.83, 185.87, and 204.50 mg g^{-1} at 298, 308, and 318 K, respectively. The kinetics of CV adsorption followed pseudo-second-order model ($R^2 > 0.9984$) and the chemisorption was proved to be rate-limiting step. Thermodynamic parameters, the change of free energy (ΔG°), entropy (ΔS°) and enthalpy (ΔH°), showed that the adsorption of CV on H_2dtoaCu was feasible, spontaneous and endothermic process. Here we concluded that H_2dtoaCu is a promising adsorbent for the removal of harmful dyes from aqueous solution. © 2013 Wiley Periodicals, Inc. J. Appl. Polym. Sci. 129: 2857–2864, 2013

KEYWORDS: adsorption; dyes/pigments; porous materials

Received 25 September 2012; accepted 9 January 2013; published online 6 February 2013
DOI: 10.1002/app.39009

INTRODUCTION

Recently, environmental contaminations by synthetic dyes have become a serious problem due to their negative ecotoxicological effects and bioaccumulation in wildlife. Most of these dyes are toxic, mutagenic, and carcinogenic. They are extensively used in industries such as textile, paint, acrylic, cosmetics, leather, pharmaceutical, which generate a considerable amount of colored wastewater. It is difficult to degrade dyes because they have complex structure and most of them contain aromatic rings, which make them mutagenic and carcinogenic.[1–3] The color in water bodies reduces light penetration and photosynthesis, therefore, affects the aquatic life. Moreover, dyes are one of esthetic pollution and eutrophication sources. So it is highly desirable to remove dyes from water/wastewater before discharging. Various techniques such as chemical precipitation,[4] coagulation,[5] biochemical degradation,[6] solvent extraction,[7] sonochemical degradation,[8] photocatalytic degradation,[9] micellar enhanced ultrafiltration,[10] electrochemical degradation,[11] ozone oxidation,[12,13] ion exchange,[14–16] and adsorption[2,17–27] etc., are used to remove dyes from wastewater. Among them, adsorption has been recognized as a reliable alternative due to its ease of operation, simplicity of design, high efficiency, insensitivity of toxic substances and comparable low cost of application in decoloration process. Lots of nonconventional, low-cost and easily obtainable adsorbents have been tested for dye removal such as activated carbons, clay minerals, biomaterial, and solid wastes. After the adsorbent is saturated with the dye molecules, regeneration and reuse of the adsorbent using the methods of thermal treatment, solvent extracting, acid/alkali solution eluting or oxidation etc., is necessarily for cost reduction.

Metal-organic frameworks (MOFs), which are crystalline nanoporous materials consist of metal ions joined by a variety of rigid-rod-like organic ligands through strong covalent bonds,[28,29] have received an increasing interest. This type structure not only provides MOFs with tunable options, organic functionality, high thermal and mechanical stability, open metal sites in the skeleton, large pore sizes, and high surface areas,[30,31] but also can be easily prepared in a one-pot. Because of these fascinating features, they have been widely applied in gas storage,[32] separation,[33] imaging,[34] catalysis,[35,36] and drug

Applied Polymer SCIENCE

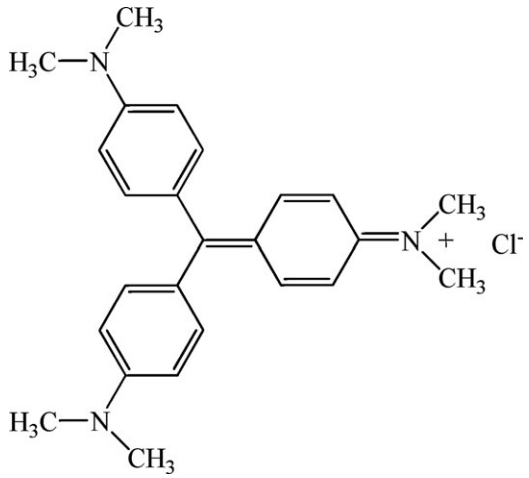

Scheme 1. The structure of crystal violet.

delivery.[34,37] Besides, the adsorptive removal of hazardous materials has also been studied using MOFs. For examples, adsorption of hydrogen sulfide from waste gases were carried out on MIL-53 (Al, Cr, Fe), MIL-47 (V), MIL-100 (Cr), and MIL-101 (Cr).[38] The applications of MOFs based on chromium-benzenedicarboxylates for the adsorptive removal of methyl orange from aqueous solution[39] and the applications of MOF-235 for the removal of methyl orange and methylene blue from contaminated water have also been reported.[40] However, to the best of our knowledge, no study on the adsorptive removal of hazardous materials using copper coordination polymer with dithiooxamide (H_2dtoaCu), one of the metal-organic frameworks (MOFs) material, is available.

Crystal violet (CV) is one of synthetic basic cationic dye, which has been shown to have detrimental effects on living organisms on short periods of exposure. The purpose of this study is to explore the potential application of H_2dtoaCu in the adsorption removal of CV from aqueous solution. The effects of various operating parameters such as initial pH, adsorbent concentration, temperature, contact time and initial dye concentration on dye removal were investigated. Then the adsorption isotherms and kinetics of adsorption of CV were studied. In addition, the thermodynamic parameters were calculated for the CV adsorption on the adsorbent.

EXPERIMENTAL

Reagents and Equipments

All chemical reagents were of analytical grade and used without further purification. The crystal violet (Scheme 1) was purchased from Sigma–Aldrich Company. The stock solution (1000 mg mL^{-1}) of CV was prepared by dissolving the desired amount of the CV in acetonitrile. All working solutions were prepared through diluting of the stock solution with distilled water. The ligand, dithiooxamide, NH_2—C(S)—C(S)—NH_2, abbreviated as H_2dtoaH_2, was purchased from International Laboratory, USA. Copper(II) sulfate pentahydrate, $CuSO_4$, was purchased from commercial sources and used as received.

The UV–vis measurements were carried out on a Lambela 750 spectrometer from Perkin Elmer. The centrifugations of sample

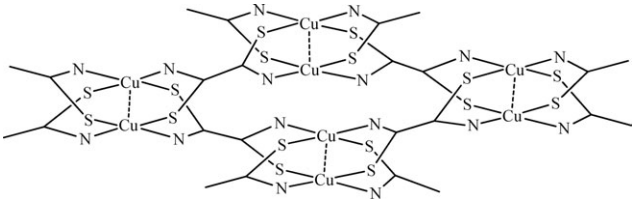

Scheme 2. The structure of H_2dtoaCu (H is omitted for the sake of clarity).[41,42]

were carried out by a TG16-W Tracfe high-speed centrifuge. The pH measurements were made using a pH meter (Model pHS-3C, Dapu instrument, Shanghai).

The quality of synthesized H_2dtoaCu sample was checked by powder X-ray diffraction (XRD) and IR spectroscopy. The XRD pattern of H_2dtoaCu were obtained by a Rigaku MiniFlex II desktop X-ray diffractometer with Cu Kα radiation ($\lambda = 1.5406$ nm) at 30 kV and 15 mA in steps of 0.02° (2θ) min^{-1} from 5° to 45° (2θ). Fourier transform infrared (FTIR) spectrum was measured on a Thermo Scientific Nicolet 6700 FT-IR spectrometer.

Preparation of Copper Coordination Polymer with Dithiooxamide

Copper coordination polymer with dithiooxamide (H_2dtoaCu, Scheme 2) was synthesized according to previous report procedures.[41,42] Briefly, 5% H_2dtoaH_2 ethanol solution was added to lukewarm $CuSO_4$ aqueous solution with stirring. The black precipitate was washed with water and ethanol several times, and then separated from the supernatant fraction with the centrifuge. The gelatinous precipitate was centrifugated and dried in an evacuated desiccator at 60°C till constant weight.

Adsorption Studies

To estimate the applicability of H_2dtoaCu as adsorbent for dye aqueous solution treatment, adsorption test was performed using CV as the adsorbate. Batch adsorption experiments were conducted at room temperature and used to evaluate the effects of various parameters on CV adsorption by adsorbent. The experiments were conducted with 5 mL dye solution of desired concentration. The influence of initial pH on the adsorption process was studied over a pH range of 3.0–12.0, being adjusted using 0.1 mol L^{-1} HCl or 0.1 mol L^{-1} NaOH. Then, the effect of adsorbent concentration was studied in the range from 0.2 to 2.0 mg mL^{-1} at optimum pH. For adsorption equilibrium experiments, dye solutions of different concentrations (100–700 mg L^{-1}) were shaken with the known amount of adsorbent (1.2 mg mL^{-1}) at different temperatures (298, 308, and 318 K) till the equilibrium achieved. The kinetics of adsorption was determined by analyzing the adsorptive uptake of the dye from aqueous solution at different time intervals. Three different initial concentrations of dye, viz., 50, 80, and 100 mg L^{-1}, were used for the kinetic study. After the adsorption process, the solutions were centrifuged for 10 min at 8000 rpm and the supernatants were analyzed to determine the remaining dye concentration in the solution by using a UV–vis spectrophotometer. The amount of the dye adsorbed onto the samples was determined according

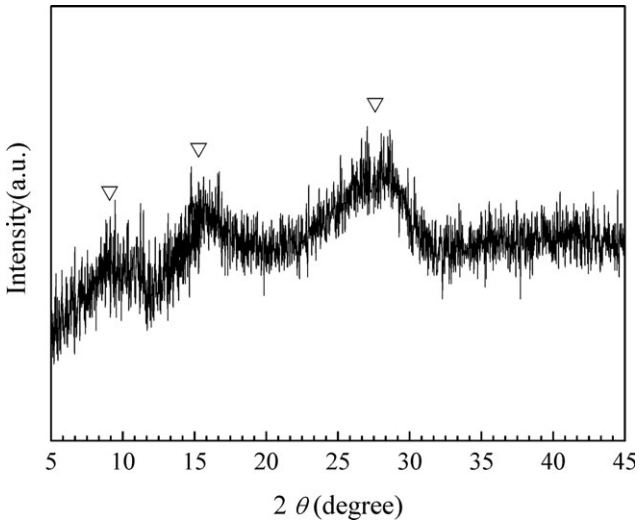

Figure 1. XRD pattern of H_2*dtoa*Cu.

to the change of concentration before and after adsorption. The amount of dye absorbed at equilibrium, q_e (mg g^{-1}), was obtained by:

$$q_e = \frac{(C_i - C_e)V}{W} \quad (1)$$

where C_i and C_e are the liquid-phase concentrations of dye at initial and equilibrium, respectively (mg L^{-1}). V is the volume of the solution (L) and W is the weight of adsorbent used (g).

The removal percentage (%) of dye was calculated using the following equation:

$$\text{Dye removal } (\%) = \frac{(C_i - C_e)}{C_i} \times 100 \quad (2)$$

RESULTS AND DISCUSSION

Characterization of H_2*dtoa*Cu

Figure 1 illustrates the XRD pattern of H_2*dtoa*Cu. Three characteristic peaks for H_2*dtoa*Cu ($2\theta \approx 9.0°$, 15.4°, and 27.6°), corresponding to interplanar distance of (9.83, 5.75, 3.23 nm), were observed in the samples.[41] The crystal structure of the polymer H_2*dtoa*Cu was revealed to be a two dimensional framework with Cu-dimeric units and bridging ligands as shown in Scheme 1. The IR spectrum of the polymer H_2*dtoa*Cu is shown in Figure 2. The strong absorption band at 3241 cm^{-1} was attributable to the sum of the contribution from the O—H stretching vibration and N—H stretching vibration. The peaks of 1613 and 1501 cm^{-1} might represent N—H bending band and NH_2 wagging and twisting band, respectively. The C—N stretching band appeared at 1311 cm^{-1}. Other peaks (1113, 1049, 955, 860, 786, and 620 cm^{-1}) were also observed, which might be attribute to C—C stretching, C—S stretching and C—H blending. All these peaks had been founded in the spectrum of the identical polymer (H_2*dtoa*Cu) synthesized by Kanda et al.[41] The XRD and IR results indicated that the polymer was successfully synthesized under the experimental condition.

Effect of Initial pH

Previous studies showed that the initial solution pH was an important parameter in the adsorption process.[17–19] To establish the effect of initial solution pH on CV adsorption on H_2*dtoa*Cu, the batch experiments were carried out at 40 mg L^{-1} initial dye concentration with adsorbent concentration of 1.6 mg mL^{-1} at 298 K for 100 min equilibrium time (Figure 3). It was found that the percentage of CV removal increased with the increasing of pH value and reached the maximum at pH = 11. Thus, alkaline solutions were used for further experiments as they lead to maximum removal of the dye.

The increase of CV removal with increasing pH suggests that the adsorption might be partly due to the presence of excess H^+ ions competing with dye cations for the adsorption sites. In

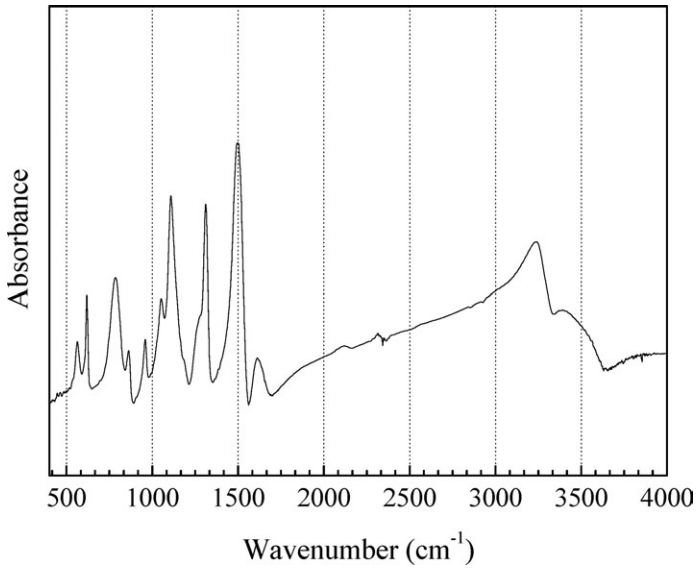

Figure 2. IR spectrum of H_2*dtoa*Cu.

Applied Polymer SCIENCE

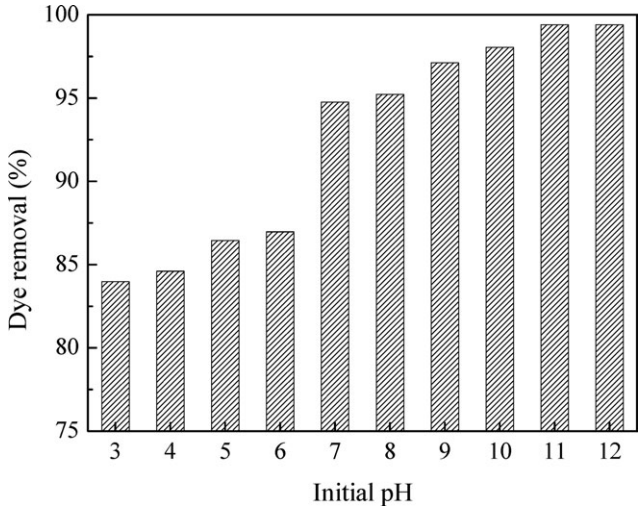

Figure 3. Effect of initial pH on the adsorption of CV onto H_2*dtoa*Cu (initial dye concentration = 40 mg L^{-1}, adsorbent concentration = 1.6 mg mL^{-1}, contact time = 100 min, temperature = 298 K).

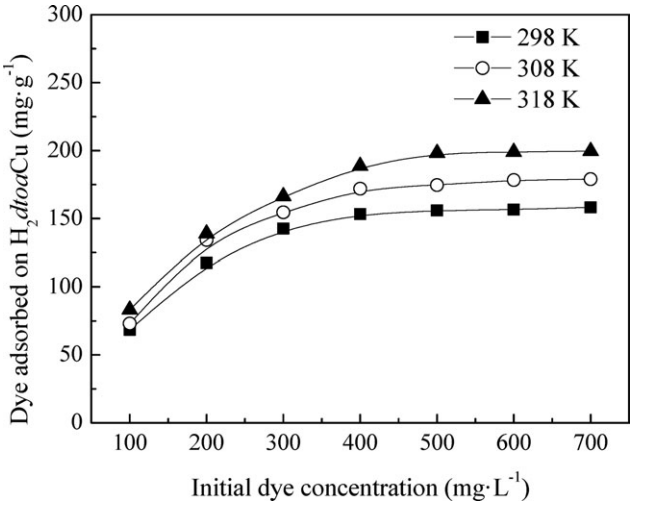

Figure 5. Effect of temperature on the adsorption of CV onto H_2*dtoa*Cu (adsorbent concentration = 1.2 mg mL^{-1}, contact time = 360 min, pH = 11).

addition, as the pH of the solution increased, the number of negatively charged surface sites increased and the number of positively charged surface sites decreased on H_2*dtoa*Cu, which favored the adsorption of dye cationic due to electrostatic interaction.[17] A similar phenomenon has been reported for the adsorption of cationic dyes, methyl blue, on MOF-235 and the electrostatic interaction between methyl blue and adsorbent was proposed.[40]

Effect of Adsorbent Concentration

Figure 4 shows the effect of adsorbent concentration on the removal of CV onto H_2*dtoa*Cu. It was observed that the percentage of dye removal increased with the increasing of adsorbent concentration and reached an equilibrium value after 1.2 mg mL^{-1}. This could be attributed to an increase in the adsorbent surface area, augmenting the number of adsorption sites available for adsorption. Under the constant dye concentration and volume, we can observe the reduction in the amount of dye adsorbed on H_2*dtoa*Cu with further increasing concentration of adsorbent. This may be caused by overlapping or aggregation of adsorption sites resulting in decrease in total adsorbent surface area available to dye and an increase in diffusion path length. These observations are in agreement with those reported previously by other researchers for the sorption of dyes by different materials.[18,19] Therefore, in the following experiments, the adsorbent concentration was fixed at 1.2 mg mL^{-1}.

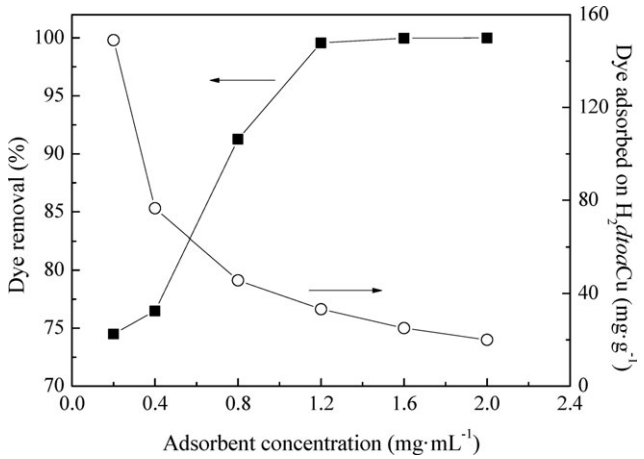

Figure 4. Effect of adsorbent concentration on the adsorption of CV onto H_2*dtoa*Cu (initial dye concentration = 40 mg L^{-1}, contact time = 100 min, temperature = 298 K, pH = 11).

Effect of Temperature

The effect of temperature was studied with initial CV concentrations ranging from 100 to 700 mg L^{-1} and 1.2 mg mL^{-1} adsorbent at 298–318 K. Figure 5 shows the CV adsorbed on H_2*dtoa*Cu versus initial CV concentrations at 298, 308, and 318 K, respectively. It can be seen the equilibrium adsorption uptakes increased with increasing temperature at all concentrations studied, which indicated that the adsorption process was endothermic.

Effect of Contact Time and Initial Dye Concentration

Figure 6 represents the dye adsorbed on H_2*dtoa*Cu versus the contact time for different initial dye concentrations (50, 80, and 100 mg L^{-1}) with adsorbent concentration of 1.2 mg mL^{-1} at 298 K. It showed that adsorption of CV on H_2*dtoa*Cu was fast and the equilibrium was achieved by 100 min of contact time. The adsorption was faster at the beginning due to the abundant availability of active sites on the H_2*dtoa*Cu surface. Afterwards with the gradual occupancy of the active sites, the adsorption became less efficient. The results also showed that an increase in the initial dye concentration led to an increase in the amount of dye adsorbed on H_2*dtoa*Cu. The amount of dye adsorbed on H_2*dtoa*Cu at equilibrium increased from 37.71 to 68.01 mg g^{-1} with an increase in the initial CV concentrations from 50 to 100 mg L^{-1}. The reason maybe lies in that an increase in initial CV concentration enhanced the driving force of the concentration gradient. Similar observations have been reported for the adsorption of dyes on other adsorbents, such as adsorption of

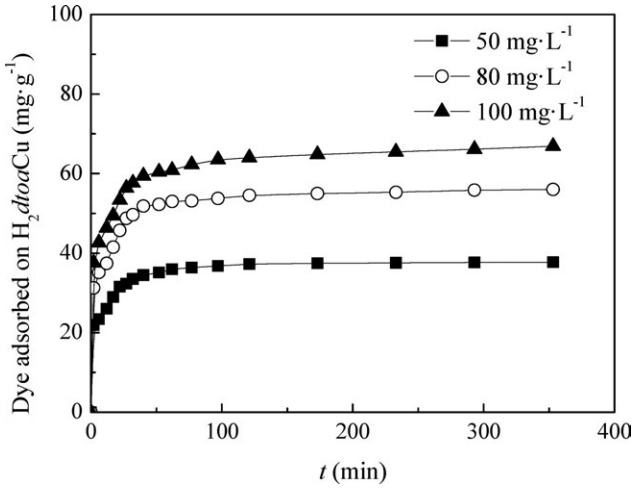

Figure 6. Effect of contact time and initial dye concentration on the adsorption of CV onto H_2*dtoa*Cu (adsorbent concentration = 1.2 mg mL^{-1}, temperature = 298 K, pH = 11).

acid dye onto durian peel,[17] malachite green dye onto agro-industry waste,[18] methylene blue and CV onto palm kernel fiber,[19] and methyl violet onto holloysite nonotubes.[20]

Adsorption Isotherms

The equilibrium adsorption isotherm models are fundamental in describing the interactive behavior between adsorbate and adsorbents, and important for investigating the mechanisms of adsorption. In this study, the Langmuir[43] and Freundlich[44] models were used to describe the adsorption equilibrium data derived from the adsorption of CV by H_2*dtoa*Cu at different temperatures.

The Langmuir isotherm model assumes monolayer sorption on a surface with a finite number of identical sites.[43] The linear form of Langmuir is represented as follows:

$$\frac{C_e}{q_e} = \frac{C_e}{q_m} + \frac{1}{K_L q_m} \tag{3}$$

where C_e is the liquid-phase concentration of dye at equilibrium (mg L^{-1}), q_e is the amount of dye absorbed at equilibrium (mg g^{-1}), q_m is the theoretical maximum adsorption capacity corresponding to monolayer coverage (mg g^{-1}), and K_L is the Langmuir isotherm constant (L mg^{-1}). The linear plots of C_e/q_e versus C_e are shown in Figure 7(a) and the parameters are shown in Table I. All the correlation coefficients for the isotherms were higher than 0.9983 ($R^2 > 0.9983$) at the three temperatures, indicating that the adsorption of CV on H_2*dtoa*Cu can be best described by the Langmuir isotherm model. The maximum monolayer adsorption capacities of H_2*dtoa*Cu increased with increasing temperature, which were 165.83 mg g^{-1} at 298 K, 185.87 mg g^{-1} at 308 K and 204.50 mg g^{-1} at 318 K, respectively.

To study whether the adsorption process is favorable or not, a dimensionless constant separation factor R_L is defined. It says that the adsorption process is irreversible when R_L is 0; favorable when R_L is between 0 and 1; linear when R_L is 1; and unfavorable when R_L is greater than 1. R_L is defined as:[17]

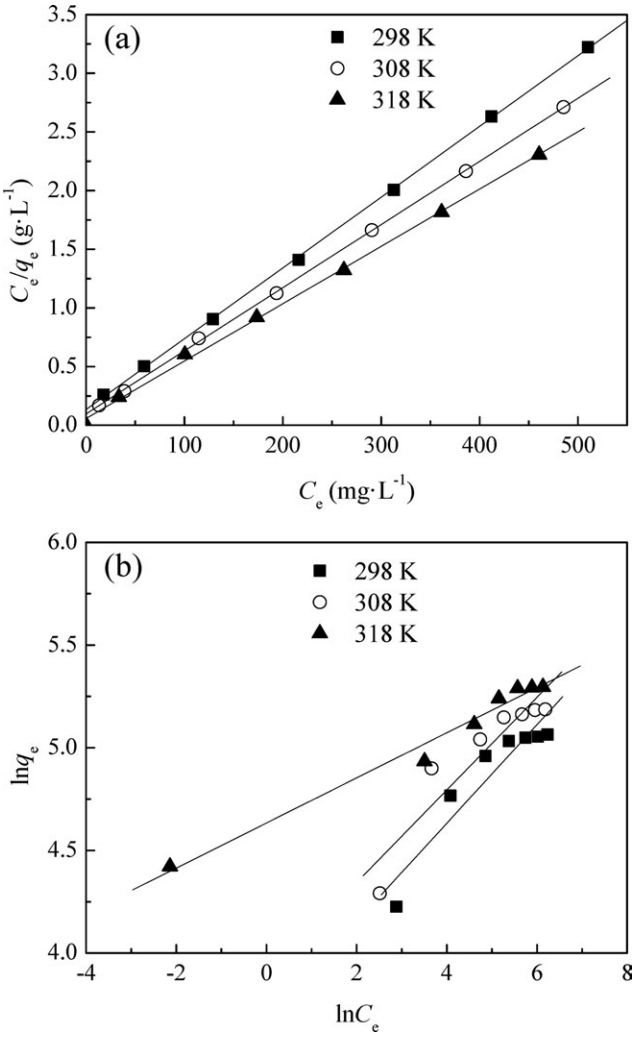

Figure 7. Adsorption isotherm models for CV adsorption onto H_2*dtoa*Cu (a) Langmuir isotherm model (b) Freundlich isotherm model.

$$R_L = \frac{1}{1 + K_L C_i} \tag{4}$$

where C_i is the initial dye concentration (mg L^{-1}), and K_L is the Langmuir isotherm constant (L mg^{-1}). The calculated values of R_L were all in the range of 0.017–0.184 (Table I), thereby confirmed that the three adsorption processes were all favorable at the temperature studied.

The Freundlich isotherm model is used for heterogeneous surface energies, in which the energy term in the Langmuir equation varies as a function of the surface coverage strictly due to variations in the heat of adsorption.[44] Freundlich model can be represented by the linear form as follows[17]:

$$\ln q_e = \ln K_F + \left(\frac{1}{n}\right) \ln C_e \tag{5}$$

where C_e is the liquid-phase concentrations of dye at equilibrium (mg L^{-1}), q_e is the amount of dye absorbed at equilibrium

Table I. Adsorption Isotherm Constants for Adsorption of CV on H_2dtoaCu at Different Temperatures

	Langmuir isotherm parameters				Freundlich isotherm parameters		
T (K)	q_m (mg g^{-1})	K_L (L mg^{-1})	R_L	R^2	K_F (mg g^{-1}) (L mg^{-1})$^{1/n}$	n	R^2
298	165.83	0.0444	0.031–0.184	0.9998	39.36	4.17	0.8882
308	185.87	0.0556	0.025–0.152	0.9998	49.05	4.44	0.8655
318	204.50	0.0832	0.017–0.107	0.9983	102.86	9.10	0.9802

(mg g^{-1}). K_F is Freundlich constant (mg g^{-1})(L mg^{-1})$^{1/n}$ and $1/n$ is the adsorption intensity. In general, as the K_F increases the adsorption capacity of adsorbent for a given adsorbate increases. The magnitude of the exponent, $1/n$, gives an indication of the favorability of adsorption. Values of $n > 1$ represent favorable adsorption condition.[17,45] The linear of lnq_e versus lnC_e at different temperatures are shown in Figure 7(b) and the parameters are summarized in Table I. The values of Freundlich exponent n range from 4.17 to 9.10, indicate the favorable adsorption. Its correlation coefficients ($0.8655 < R^2 < 0.9802$) is much lower than that for the Langmuir isotherm, suggesting that Langmuir isotherm model yields a much better fit than the Freundlich model. The results indicate the monolayer coverage of dyes onto particles and also the homogenous distribution of active sites on H_2dtoaCu.

To assess the potential of H_2dtoaCu, a comparative evaluation of the adsorption capacities of various types of adsorbents for the sorption of basic dyes is shown in Table II. The monolayer equilibrium capacities of H_2dtoaCu are larger than most of the other types of adsorbents, indicating that H_2dtoaCu is an effective adsorbent for CV removal from aqueous solution.

Table II. Comparison of Monolayer Equilibrium Capacities of Various Types of Adsorbents for CV Adsorption

Adsorbents	q_e (mg g^{-1})	Reference
Semi-interpenetrated networks hydrogels	35.1	Li et al.[2]
Palm kernel fiber	78.9	Garg et al.[18]
Polyacrylic acid-bound magnetic nanoparticles	116	Liao et al.[21]
Tomato plant root	94.3	Kannan et al.[22]
Phosphoric acid activated carbon	60.4	Senthilkumaar et al.[23]
Cu(II)-loaded montmorillonite	114.3	Wang et al.[24]
NaOH-modified rice husk	34.0–44.9	Chakraborty et al.[25]
Manganese oxide-coated sepiolite	319	Eren et al.[26]
H_2dtoaCu	165.83–204.50	This study

Kinetics Studies

To identify the mechanism and the potential rate controlling steps involved in the adsorption of CV onto H_2dtoaCu, two kinetic models, pseudo-first-order and pseudo-second-order were studied and adopted to investigate the adsorption process. The best-fit model was selected based on the linear regression correlation coefficient values (R^2).

The pseudo-first-order kinetic model equation can be represented as follows[20]:

$$\log(q_e - q_t) = \log q_e - \frac{k_1}{2.303} t \tag{6}$$

The pseudo-second-order kinetic model equation can be represented as follows[20]:

$$\frac{t}{q_t} = \frac{1}{k_2 q_e^2} + \frac{t}{q_e} \tag{7}$$

where q_e is the amount of dye absorbed at equilibrium (mg g^{-1}), q_t is the amount of dye adsorbed at time t (mg g^{-1}), k_1 is the pseudo-first-order rate constant (min^{-1}) and k_2 is the pseudo-second-order rate constant (g·(mg min)$^{-1}$).

Pseudo-first-order and pseudo-second-order kinetic parameters of CV adsorption onto H_2dtoaCu for different initial dye concentrations are summarized in Table III, and plots of pseudo-first-order and pseudo-second-order kinetic models are shown in Figure 8. The results showed that the correlation coefficients (R^2), obtained at different initial dye concentrations for the pseudo-first-order kinetic model, were in the range of 0.8658–0.9616. In addition, the theoretical and experimental equilibrium adsorption capacities, q_e obtained from this kinetic model varied widely. These findings suggest that adsorption of CV on H_2dtoaCu cannot be described by the pseudo-first-order kinetic model. Conversely, the kinetic data exhibited an excellent compliance with pseudo-second-order kinetic equation. The plots of t/q_t against t of different initial dye concentrations showed excellent linearity [see Figure 8(b)]. As shown in Table III, the calculated values of q_e agreed with experimental values well, and the correlation coefficients for the pseudo-second-order kinetic plots were all significantly higher than 0.9984 ($R^2 > 0.9984$). The best correlation for the system provided by the pseudo-second-order model suggests that chemisorption might be rate-limiting step for the sorption of CV onto H_2dtoaCu.[46] It was likely that the adsorption behavior may involve valence forces

Table III. Kinetic Parameters for Adsorption of CV on H_2*dtoa*Cu at Different Initial Dye Concentrations

		Pseudo-first-order kinetic model			Pseudo-second-order kinetic model		
C_i (mg L^{-1})	$q_{e,exp}$ (mg g^{-1})	$q_{e,cal}$ (mg g^{-1})	k_1 (min^{-1})	R^2	$q_{e,cal}$ (mg g^{-1})	$k_2 \times 10^3$ (g (mg $min^{-1})^{-1}$)	R^2
50	37.71	14.11	0.0311	0.9616	38.24	6.1	0.9987
80	56.70	19.91	0.0241	0.8658	56.09	4.3	0.9984
100	68.01	24.45	0.0198	0.9153	65.49	3.7	0.9986

through sharing or exchange of electrons between adsorbent and adsorbate.

The pseudo-second-order rate constants for adsorption of CV over H_2*dtoa*Cu (3.7×10^{-3} –6.1×10^{-3} g (mg $min^{-1})^{-1}$) are larger than those over most of the other reported adsorbents, e.g., Palm kernel fiber (0.35×10^{-3} g·(mg $min^{-1})^{-1}$,[19] Cu(II)-loaded montmorillonite (3.5×10^{-3} g·(mg $min^{-1})^{-1}$),[24] NaOH-modified rice husk (0.62×10^{-3}–2.32×10^{-3} g·(mg $min^{-1})^{-1}$),[25] and manganese oxide-coated sepiolite (0.15×10^{-3}–1.47×10^{-3} g·(mg $min^{-1})^{-1}$).[26] The kinetic constants over H_2*dtoa*Cu decrease slightly with increasing the initial CV concentration. Similar tendency have been reported for the adsorption of CV on Palm kernel fiber[19] and manganese oxide-coated sepiolite.[26] In the condition of lower concentrations, CV present in the aqueous solution could interact with the binding sites, hence a higher rate constant results. Whereas in the condition of higher concentrations, the rate constant of dye adsorption onto the H_2*dtoa*Cu shows a decreasing trend because of the saturation of the adsorption sites. After the initial stage of adsorption, it is difficult for the remaining vacant surface sites to be occupied due to repulsive forces between the CV molecules on the H_2*dtoa*Cu surface.[26]

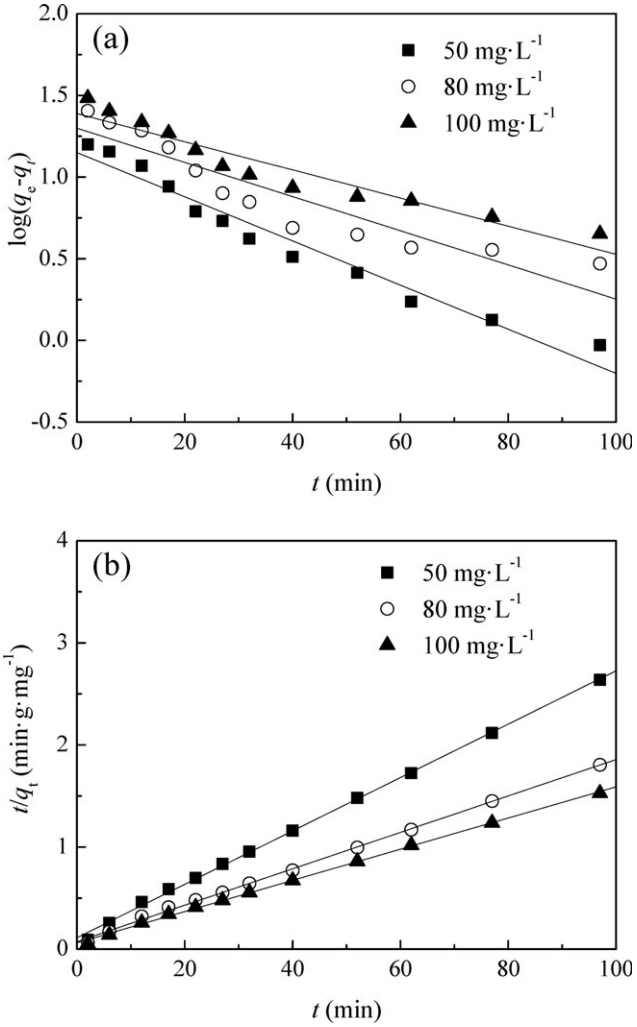

Figure 8. Plots of (a) pseudo-first-order and (b) pseudo-second-order kinetic models for CV adsorption onto H_2*dtoa*Cu at different initial dye concentrations.

Evaluation of Adsorption Thermodynamics

The increase in adsorption at higher temperature revealed an endothermic process which can be explained thermodynamically by evaluating parameters, such as change in free energy (ΔG°), entropy (ΔS°) and enthalpy (ΔH°). These parameters were calculated using the following equations[39,40]:

$$\Delta G^\circ = -RT \ln K_L \quad (8)$$

$$\ln K_L = \frac{\Delta S^\circ}{R} - \frac{\Delta H^\circ}{RT} \quad (9)$$

where R is the gas constant (8.314 J (mol $K^{-1})^{-1}$). K_L is Langmuir isotherm constant (dimension: L mol^{-1}), ΔG° is Gibbs free energy change (kJ mol^{-1}), ΔH° is enthalpy of reaction (kJ mol^{-1}) and ΔS° is entropy of reaction (J (mol $K^{-1})^{-1}$). K_L can be obtained from the slope/intercept of the Langmuir plot of Figure 7(a). The negative values of Gibbs free energy change (ΔG°) shown in Table IV, indicated a feasible and spontaneous process.[17] ΔS° and ΔH° can be determined from the slope and the intercept of the linear plot of $\ln K_L$ versus $1/T$ and the results are also shown in Table IV. It was found that the positive value of entropy (ΔS° = 102.66 J (mol $K^{-1})^{-1}$) represented an

Table IV. Thermodynamic Parameters for CV Adsorption on the H_2*dtoa*Cu

T (K)	K_L (L mol^{-1})	ΔG° (kJ mol^{-1})	ΔS°(J (mol $K^{-1})^{-1}$)	ΔH° (kJ mol^{-1})
298	18.11	−5.85	102.66	24.74
308	22.68	−6.87		
318	33.94	−7.89		

increasing in degree of freedom or in the disorder of adsorption process. The high positive value of enthalpy (ΔH°), 24.74 kJ mol^{-1}, confirmed the endothermic nature of the overall adsorption process. This means that as the temperature increases, more energy is available to enhance the adsorption and the adsorption capacity also increases (as shown in Figure 5).[27]

CONCLUSIONS

Here we demonstrated the adsorption of crystal violet from aqueous solution onto a MOFs material, copper coordination polymer with dithiooxamide (H_2*dtoa*Cu). Adsorption isotherms and kinetics were determined, and the results showed that Langmuir adsorption isotherm and pseudo-second-order kinetic model matched well for the adsorption of crystal violet onto H_2*dtoa*Cu. Values of thermodynamic parameters such as the change of free energy, enthalpy, and entropy of adsorption were determined, indicating that the adsorption was feasible, spontaneous and endothermic process in nature. Based on these studies, H_2*dtoa*Cu was confirmed to be a promising adsorbent for the removal of harmful dyes from aqueous solution.

REFERENCES

1. Hao, O. J.; Kim, H.; Chiang, P. C. *Crit. Rev. Environ. Sci. Technol.* **2000**, *30*, 449.
2. Li, S. *Bioresour. Technol.* **2010**, *101*, 2197.
3. Robinson, T.; McMullan, G.; Marchant, R.; Nigam, P. *Bioresour. Technol.* **2001**, *77*, 247.
4. Tan, B. H.; Teng, T. T.; Omar, A. K. M. *Water Res.* **2000**, *34*, 597.
5. Lee, J. W.; Choi, S. P.; Thiruvenkatachari, R.; Shim, W. G.; Moon, H. *Water Res.* **2006**, *40*, 435.
6. Kagalkar, A. N.; Jagtap, U. B.; Jadhav, J. P.; Bapat, V. A.; Govindwar, S. P. *Bioresour. Technol.* **2009**, *100*, 4104.
7. Lee, D. W.; Hong, W. H.; Hwang, K. Y. *Sep. Sci. Technol.* **2000**, *35*, 1951.
8. Hong, Q.; Hardcastle, J. L.; McKeown, R. A. J.; Marken, F.; Compton, R. G. *N. J. Chem.* **1999**, *23*, 845.
9. Muruganandham, M.; Swaminathan, M. *J. Hazard Mater.* **2006**, *135*, 78.
10. Purkait, M. K.; DasGupta, S.; De, S. *Sep. Purif. Technol.* **2004**, *37*, 81.
11. Fernandes, A.; Morão, A.; Magrinho, M.; Lopes, A.; Gonçalves, I. *Dyes Pigment* **2004**, *61*, 287.
12. Mao, Y. H.; Guan, Y.; Luo, D. H.; Zheng, Q. K.; Feng, X. N.; Wang, X. X. *Color Technol.* **2011**, *127*, 256.
13. Eren, H. A.; Ozturk, D.; Eren, S. *Color Technol.* **2011**, *128*, 75.
14. Wawrzkiewicz, M. *Ind. Eng. Chem. Res.* **2012**, *51*, 8069.
15. Wawrzkiewicz, M. *Solvent Extr. Ion. Exch.* **2010**, *28*, 845.
16. Liu, C. H.; Wu, J. S.; Chiu, H. C.; Suen, S. Y.; Chu, K. H. *Water Res.* **2007**, *41*, 1491.
17. Hameed, B. H.; Hakimi, H. *Biochem. Eng. J.* **2008**, *39*, 338.
18. Garg, V. K.; Kumar, R.; Gupta, R. *Dyes Pigment* **2004**, *62*, 1.
19. El-Sayed, G. O. *Desalination* **2011**, *272*, 225.
20. Liu, R.; Zhang, B.; Mei, D.; Zhang, H.; Liu, J. *Desalination* **2011**, *268*, 111.
21. Liao, M. H.; Wu, K. Y.; Chen, D. H. *Sep. Purif. Technol.* **2005**, *39*, 1563.
22. Kannan, C.; Buvaneswari, N.; Palvannan, T. *Desalination* **2009**, *249*, 1132.
23. Senthilkumaar, S.; Kalaamani, P.; Subburaam, C. V. *J. Hazard Mater.* **2006**, *136*, 800.
24. Wang, X. S.; Zhang, W. *Sep. Purif. Technol.* **2011**, *46*, 656.
25. Chakraborty, S.; Chowdhury, S.; Das Saha, P. *Carbohydr. Polym.* **2011**, *86*, 1533.
26. Eren, E.; Cubuk, O.; Ciftci, H.; Eren, B.; Caglar, B. *Desalination* **2010**, *252*, 88.
27. Gercel, O.; Gercel, H. F.; Savas Koparal, A.; Ogutverenc, U. B. *J. Hazard. Mater.* **2008**, *160*, 668.
28. Li, H.; Eddaoudi, M.; O'Keeffe, M.; Yaghi, O. M. *Nature* **1999**, *402*, 276.
29. Rowsell, J.; Yaghi, O. M. *Microporous. Mesoporous. Mater.* **2004**, *73*, 3.
30. Férey, G. *Chem. Soc. Rev.* **2008**, *37*, 191.
31. Yaghi, O. M.; O'Keeffe, M.; Ockwig, N. W.; Chae, H. K.; Eddaoudi, M.; Kim, J. *Nature* **2003**, *423*, 705.
32. Vitillo, J. G.; Regli, L.; Chavan, S.; Ricchiardi, G.; Spoto, G.; Dietzel, P. D. C.; Bordiga, S.; Zecchina, A. *J. Am. Chem. Soc.* **2008**, *130*, 8386.
33. Bastin, L.; Barcia, P. S.; Hurtado, E. J.; Silva, J. A. C.; Rodrigues, A. E.; Chen, B. *J. Phys. Chem. C* **2008**, *112*, 1575.
34. Pashow, K. M. L.; Rocca, J. D.; Xie, Z. G.; Tran, S.; Lin, W. B. *J. Am. Chem. Soc.* **2009**, *131*, 14261.
35. Ma, L. Q.; Falkowski, J. M.; Abney, C.; Lin, W. B. *Nat. Chem.* **2010**, *2*, 838.
36. Alaerts, L.; Seguin, E.; Poelman, H.; Thibault-Starzyk, F.; Jacobs, P. A. *Chem. Eur. J.* **2006**, *12*, 7353.
37. Horcajada, P.; Serre, C.; Vallet-Regi, M.; Sebban, M.; Taulelle, F.; Férey, G. *Angew. Chem.* **2006**, *45*, 5974.
38. Hamon, L.; Serre, C.; Devic, T.; Loiseau, T.; Millange, F.; Férey, G.; Weireld, G. D. *J. Am. Chem. Soc.* **2009**, *131*, 8775.
39. Haque, E.; Lee, J. E.; Jang, I. T.; Hwang, Y. K.; Chang, J. S.; Jegal, J.; Jhung, S. H. *J. Hazard. Mater.* **2010**, *181*, 535.
40. Haque, E.; Jun, J. W.; Jhung, S. H. *J. Hazard. Mater.* **2011**, *185*, 507.
41. Kanda, S.; Suzuki, A.; Ohkawa, K. *Ind. Eng. Chem. Prod. Res. Dev.* **1973**, *12*, 88.
42. Kitagawa, H.; Nagao, Y.; Fujishima, M.; Ikeda, R.; Kanda, S. *Inorg. Chem. Commun.* **2003**, *6*, 346.
43. Langmuir, I. *J. Am. Chem. Soc.* **1916**, *38*, 2221.
44. Freundlich, H. M. F. *Z. Phys. Chem.* **1906**, *57*, 385.
45. Treybal, R. E. Mass Transfer Operations, 2nd ed.; McGraw Hill: New York, **1968**.
46. Ho, Y. S.; Mckay, G. *Water Res.* **2000**, *34*, 735.